frontiers in Medicine

ORIGINAL RESEARCH
published: 21 January 2022
doi: 10.3389/fmed.2021.836438

The Role of Pre-therapeutic ^{18}F-FDG PET/CT in Pediatric Hemophagocytic Lymphohistiocytosis With Epstein-Barr Virus Infection

Xia Lu[1†], Ang Wei[2†], Xu Yang[1], Jun Liu[1], Siqi Li[1], Ying Kan[1], Wei Wang[1], Tianyou Wang[2], Rui Zhang[2] and Jigang Yang[1*]*

[1] Nuclear Medicine Department, Beijing Friendship Hospital Affiliated to Capital Medical University, Beijing, China, [2] National Center for Children's Health, Hematology Center, Beijing Children's Hospital, Capital Medical University, Beijing, China

OPEN ACCESS

Edited by:
Domenico Albano,
University of Brescia, Italy

Reviewed by:
Francesco Dondi,
Università degli Studi di Brescia, Italy
Alberto Miceli,
Università di Genova, Italy

***Correspondence:**
Jigang Yang
yangjigang@ccmu.edu.cn
Rui Zhang
ruizh1973@126.com

[†]These authors have contributed equally to this work

Specialty section:
This article was submitted to Nuclear Medicine, a section of the journal Frontiers in Medicine

Received: 15 December 2021
Accepted: 30 December 2021
Published: 21 January 2022

Citation:
Lu X, Wei A, Yang X, Liu J, Li S, Kan Y, Wang W, Wang T, Zhang R and Yang J (2022) The Role of Pre-therapeutic ^{18}F-FDG PET/CT in Pediatric Hemophagocytic Lymphohistiocytosis With Epstein-Barr Virus Infection. Front. Med. 8:836438. doi: 10.3389/fmed.2021.836438

Objective: To evaluate the role of pre-therapeutic ^{18}F-FDG PET/CT in pediatric hemophagocytic lymphohistiocytosis (HLH) with Epstein-Barr virus (EBV) infection.

Methods: This retrospective study included 29 HLH children (1–16 years) with EBV infection, who underwent pre-therapeutic ^{18}F-FDG PET/CT from July 2018 to November 2020. Pathology results were considered as the reference standard. These patients were divided into two groups: EBV-induced malignancy-associated HLH (M-HLH, $N = 9$) and EBV-induced non-malignancy-associated HLH (NM-HLH, $N = 20$). The regions of interest (ROIs) of the liver, spleen (Sp), bone marrow (BM), lymph nodes (LN), hypermetabolic lesions, liver background (LiBG), and mediastinum (M) were drawn with software 3D-Slicer. The volumetric and metabolic parameters, including maximum standard uptake value (SUV_{max}), metabolic tumor volume, and total lesion glycolysis of these ROIs, clinical parameters, and laboratory parameters were compared between the two groups. The efficiency of the above parameters in predicting the treatment response and overall survival (OS) was analyzed.

Results: Receiver operating characteristic curve analysis indicated that SUV_{max}-lesions and SUV_{max}-LN/M (AUC = 0.822, 0.819, cut-off = 6.04, 5.74, respectively) performed better in differentiating M-HLH from NM-HLH. It had the best diagnostic performance when age was added with the SUV_{max}-LN/M (AUC = 0.933, sensitivity = 100%, specificity = 85.0%). The presence of extranodal hypermetabolic lesions in multiple organs indicated the M-HLH ($P = 0.022$). Older age, higher SUV_{max}-LN and SUV_{max}-lesions, and the presence of serous effusion were associated with poorer treatment response at the 2nd and 4th week (not reaching partial remission). Multivariate analysis showed that SUV_{max}-lesions > 7.66 and SUV_{max}-Sp/LiBG > 2.01 were independent prognostic factors for overall survival ($P = 0.025$, 0.036, respectively).

Conclusions: ^{18}F-FDG PET/CT could be a valuable technique for identifying the underlying malignancy and predicting prognosis in pediatric HLH with EBV infection. M-HLH could be considered when SUV_{max}-lesions > 6.04, SUV_{max}-LN/M > 5.74, and the presence of extranodal hypermetabolic lesions in multiple organs on ^{18}F-FDG PET/CT. SUV_{max}-lesions and SUV_{max}-Sp/LiBG might be independent prognostic factors for OS.

Keywords: hemophagocytic lymphohistiocytosis (HLH), Epstein-Barr virus (EBV), ^{18}F-FDG PET/CT, differential diagnosis, prognosis, children

INTRODUCTION

Hemophagocytic lymphohistiocytosis (HLH) is a clinical syndrome of uncontrolled activation of the immune system due to a variety of reasons, charactering as excessive elevated inflammatory cytokines and multiple organs damages (1). As a rare disease with poor outcomes, HLH have an estimated yearly incidence of one to ten per million children and a five-year survival rate of 54% (2, 3). HLH can be classified into two forms, primary HLH with related gene mutations, and secondary HLH associated with infection, malignancy, or autoimmune disorders (4).

The incidence of HLH with Epstein-Barr virus infection is especially high in Asia (5). In the background of EBV infection, HLH can be driven by pure EBV infection (abbreviated as EBV-HLH in the paper), chronic active EBV infection [CAEBV, which has been defined by the World Health Organization classification as lymphoproliferative disorders (LPD)], and lymphoma (6). LPD can be divided into grade 1–3, corresponding to category A1–A3 classified by Ohshima et al. (7). The LPD grade 3 is considered as malignant disorders (8). Patients with EBV-induced malignancy-associated HLH (abbreviated as M-HLH in the study, including LPD grade 3 and lymphoma) have poorer prognosis than EBV-induced non-malignancy-associated HLH (abbreviated as NM-HLH, including LPD grade 1–2 and EBV-HLH). It is reported that higher pathologic grade predicts poorer prognosis (9). M-HLH patients would die of fulminant disease progression without intensive treatment, such as aggressive immune suppression, chemotherapy, and allogeneic hematopoietic stem cell transplant (8). However, it is difficult to differentiate M-HLH from NM-HLH, owing to the high overlap of clinical manifestation.

^{18}F-FDG PET/CT is a whole-body scan widely used in many diseases, such as infection, malignant disease, and rheumatic immunity disease (10). In varieties of lymphoma, it is used in differential diagnosis, treatment decision, response evaluation and prognosis prediction (10, 11). ^{18}F-FDG PET/CT is better than conventional radiography, as it can display the extranodal lesions better and measure the metabolism in semi-quantitative analysis (12). ^{18}F-FDG PET/CT could evaluate the involved organs of potential disease in HLH and guide the biopsy of lesions (13). In HLH with EBV infection, ^{18}F-FDG PET/CT is now recommended for the detection of neoplastic lesions, as the lymph nodes and extranodal organs are usually involved, especially in M-HLH (6). Moreover, studies reported that PET/CT parameters, such as SUV_{max} spleen/mediastinum ratio, could predict prognosis of HLH (14).

We speculate that ^{18}F-FDG PET/CT plays a certain role in detecting the potential malignancy and predicting prognosis in pediatric HLH with EBV infection, which is not investigated by now. Therefore, this study mainly included two aspects, to differentiate M-HLH from NM-HLH, and to predict the treatment response and overall survival (OS) by ^{18}F-FDG PET/CT.

Abbreviations: M-HLH, EBV-induced malignancy-associated HLH; NM-HLH, EBV-induced non-malignancy-associated HLH; EBV-HLH, HLH driven by pure EBV infection; Li, liver; Sp, spleen; BM, bone marrow; LN, lymph nodes; LiBG, liver background; M, mediastinum.

MATERIALS AND METHODS

Patients

A total of 29 children (≤ 16 years old) were analyzed retrospectively. They were all newly diagnosed HLH with EBV infection and received pre-therapeutic ^{18}F-FDG PET/CT from July 2018 to November 2020. All patients met the diagnostic criteria of HLH-2004 protocol and the criteria of EBV infection (15, 16), and the latter included serological evidence of acute or active EBV infection, evidence of EBV DNA in the blood and/or EBER positive in the tissue. Patients were excluded if they had received clinical therapy, including chemotherapy, targeted therapies, or corticosteroid before the scans, or colony-stimulating factor therapy within one week. In all enrolled patients, the potential causes of HLH were diagnosed according to the pathologic findings of lymph nodes, bone marrow or lesions. Then according to the pathology results, patients were divided into two groups, M-HLH and NM-HLH. The patients were followed up until October 2021 by telephone or medical records. OS was calculated from the date of the scan to the date of death for any cause or to the date of last follow-up. The institutional ethics committee of Beijing Friendship Hospital, Capital Medical University, approved the retrospective study and waived the requirement for written informed consent (**Figure 1**).

^{18}F-FDG PET/CT Acquisition

All ^{18}F-FDG PET/CT scans were performed with a Siemens mCT PET/CT scanner (Siemens Medical Solution, Erlangen, Germany). Patients were fasted for more than 6 h, and blood glucose level was controlled at < 7.1 mmol/L, before the intravenous administration of ^{18}F-FDG (3.7 MBq/kg).

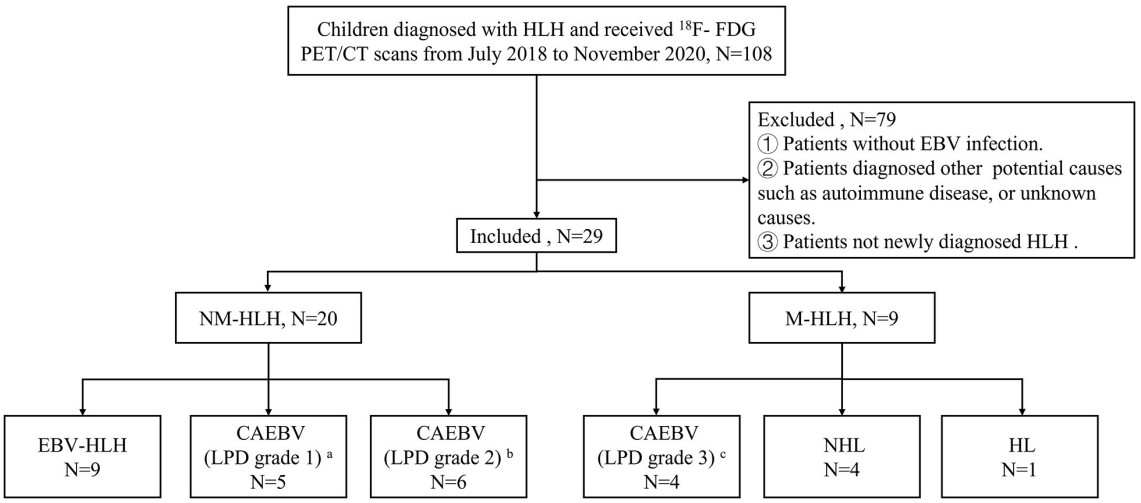

FIGURE 1 | Flow diagrams of study populations. a: category A1, b: category A2, c: category A3, in classification with the pathological categories proposed by Ohshima et al. (7). HLH, hemophagocytic lymphohistiocytosis; EBV, Epstein-Barr virus; M-HLH, EBV-induced malignancy-associated HLH; NM-HLH, EBV-induced non-malignancy-associated HLH; EBV-HLH, HLH driven by pure EBV infection; CAEBV, chronic active EBV infection; LPD, lymphoproliferative disorders; HL, Hodgkin's Lymphoma; NHL, non-Hodgkin's lymphoma.

A scan from the head to the mid-thigh was performed 60 min after injection. The CT scan was obtained at 120 kV, 200 mA and 3 mm thickness. Then PET was obtained in 3-dimensional mode at 2 min/bed. The CT-based, attenuation-corrected PET images were reconstructed with an iterative algorithm.

Image Analysis

^{18}F-FDG PET/CT images were analyzed by two experienced nuclear medicine physicians on 3D-Slicer (A free and open-source software, widely used by physicians and researchers). The whole liver, spleen and lumbar 1–5 vertebra were drawn as regions of interest (ROIs) of the liver (Li), spleen (Sp), bone marrow (BM), respectively. ROIs of lymph nodes (LN) were drawn on all lymph nodes with short diameter $>$ 0.5 cm. ROIs of lesions were drawn in all the lymph nodes and extranodal lesions. And the extranodal lesions were defined as lesions with higher FDG uptake than the background tissue in extranodal organs, excluding physiological uptake. The SUV_{max} of the liver background (LiBG) and mediastinum (M) were determined by a 3-cm spheric ROI in the liver and a circular ROI drawn within the walls of the aortic arch, respectively. Then metabolic and volumetric parameters, including maximum standard uptake value (SUV_{max}), metabolic tumor volume (MTV) and total lesion glycolysis (TLG) of these ROIs, were calculated by the software. The volumetric parameters of liver and spleen were corrected by body surface area [Du Bois (17)] and were abbreviated as MTVc and TLGc. Hypermetabolic LN, Li, Sp or BM were defined when their $SUV_{max} > 2.5$ or $SUV_{max} > SUV_{max}$-LiBG. Hepatomegaly and splenomegaly were considered when the inferior margin over the costal margin. Lymphadenopathy was considered when short-axis diameter more than 15 mm for Level II and 10 mm for others (18).

Clinical Information Review

All clinical information was reviewed from medical records, including age, gender, and laboratory results. The laboratory results were obtained within one week before the PET/CT scan, including blood routines (ANC, Hb, PLT), blood biochemical results (albumin, fibrinogen, TG, ALT, AST, LDH), serum cytokine levels (IFN-γ, TNF-α, IL-6, IL-10), serum ferritin, soluble CD25 (sCD25), NK cell activity, EBV DNA copies, ESR, and CRP.

The treatment response of HLH was assessed according to the evaluation criteria proposed by Midwest Collaboration Group of the United States and was divided into three categories: complete remission, partial remission, and no remission (19). The evaluation depended on the following quantified symptoms and laboratory markers of HLH, including levels of sCD25, serum ferritin, blood cell counts (ANC, Hb, PLT), TG, ALT, presence of hemophagocytosis in pathology specimens, and level of consciousness (in patients with central nervous system involvement).

Statistical Analysis

Data were analyzed with SPSS 26.0 (IBM, Armonk, USA) and figures were generated using GraphPad Prism 8 (GraphPad Software, San Diego, CA). Continuous variables with a skewed distribution were presented as median (range). Categorical variables were presented as numbers [percentages (%)]. Continuous variables were compared using the Mann-Whitney U test, and categorical variables were analyzed with the two-sided Fisher's exact test. Spearman correlation analysis was used for correlation analysis. The positive or negative relationship was interpretated as very high, high, moderate, low, or negligible ($|r| = 0.90–1.00$, 0.70–0.89, 0.50–0.69, 0.25–0.49, 0–0.24, respectively). Receiver operating characteristic (ROC) curves

TABLE 1 | Characteristics of patients and comparison of clinical and ^{18}F-FDG PET/CT findings between M-HLH and NM-HLH.

Parameters	Total (*N* = 29)	M-HLH (*N* = 9)	NM-HLH (*N* = 20)	*P*-value
General information				
Age (median, range)	7 (1–16)	11 (6–16)	3.5 (1–13)	0.004**
Gender (male)	14 (48.3)	4 (44.4)	10 (50.0)	1.000
Laboratory parameters (median, range)				
ANC (10^9/L)	0.91 (0.27–4.52)	1.08 (0.27–3.29)	0.91(0.28–4.52)	0.444
Hb (g/L)	96 (62–128)	107 (62–121)	95 (64–128)	0.627
PLT (10^9/L)	111 (19–211)	91 (19–201)	126 (30–211)	0.216
Fibrinogen (g/L)	1.51 (1.55–4.07)	1.62 (0.55–4.07)	1.50 (0.80–2.74)	0.982
Serum ferritin (ng/mL)	355.1 (13.2–139139.0)	317.1 (95.8–14717.6)	407.1 (13.2–139139.0)	0.945
TG (mmol/L)	2.49 (1.01–6.48)	2.86 (1.97–5.62)	2.27 (1.01–6.48)	0.183
sCD25(pg/mL)	22982 (165–218875)	36035 (5354–44000)	20169.5 (165–218875)	0.532
NK (%)	15.72 (7.21–23.83)	15.72 (7.21–19.15)	15.695 (11.54–23.83)	0.390
EBV-DNA (whole blood) (x10^5Copies/mL)	24.6 (0.0155–225)	8.1 (0.0266–109)	33.1 (0.0155–225)	0.472
EBV-DNA (plasma) (x10^5Copies/mL)	0.411 (0.005–72.8)	0.0597 (0.005–18.4)	0.0295 (0.005–72.8)	0.253
IFN-γ (pg/mL)	40.92 (2.04–625.000)	57.18 (2.04–458.51)	22.23 (2.82–625.00)	0.390
TNF-α (pg/mL)	1.78 (0.00–34.85)	1.96 (0.00–22.70)	1.21 (0.00–34.85)	0.627
IL-6 (pg/mL)	19.78 (1.80–313.98)	27.47 (1.80–128.93)	14.60 (4.37–313.98)	0.871
IL-10 (pg/mL)	22.57 (2.15–827.66)	39.40 (2.15–827.66)	21.62 (5.38–485.45)	0.908
ALT (U/L)	69.4 (5.2–439.8)	108.1 (5.2–375.3)	67.2 (11.6–439.8)	0.694
AST (U/L)	152.6 (13.2–1161.9)	236.2 (13.2–494.0)	137.1 (32.3–1161.9)	0.365
LDH (U/L)	592 (257–7527)	581 (414–3110)	605.5 (257–7527)	0.764
Albumin (g/L)	35.1 (20.0–44.1)	35.9 (27.2–39.8)	34.65 (20.0–44.1)	0.982
ESR (mm/h)	13 (2–88)	13 (2–34)	11.5 (2–88)	0.660
CRP (mg/L)	5 (5–77)	5 (5–77)	5 (5–55)	0.945
PET/CT general findings (cases, %)				
Hepatomegaly	29 (100.0)	9 (100.0)	20 (100)	1.000
Hypermetabolic Li	5 (17.2)	3 (33.3)	2 (10.0)	0.287
Splenomegaly	28 (96.6)	9 (100.0)	19 (95.0)	1.000
Hypermetabolic Sp	20 (69.0)	5 (55.6)	15 (75.0)	0.396
Lymphadenopathy	14 (16.6)	5 (55.6)	9 (45.0)	0.700
Hypermetabolic LN	25 (6.2)	9 (100.0)	16 (80.0)	0.280
Hypermetabolic BM	22 (75.9)	7 (77.8)	15 (75.0)	1.000
Serous effusion	18 (62.1)	6 (66.7)	12 (60.0)	1.000
Extranodal lesions	12 (41.4)	6 (66.7)	6 (30.0)	0.074
Extranodal lesions in multiple organs	5 (17.2)	4 (44.4)	1 (5.0)	0.022*
Metabolic parameters (median, range)				
SUV_{max}-lesions	3.49 (1.10–19.91)	8.30 (2.48–16.03)	3.10 (1.10–19.91)	0.005**
SUV_{max}-M	1.04 (0.059–1.41)	1.04 (0.059–1.34)	1.02 (0.65–1.41)	/
SUV_{max}-LiBG	1.63 (0.94–5.00)	1.80 (1.36–5.00)	1.44 (0.94–3.14)	/
SUV_{max}-LN	3.11 (1.10–16.03)	7.55 (2.48–16.03)	2.535 (1.10–19.91)	0.004**
SUV_{max}-LN/M	3.42 (1.2–16.7)	6.68 (2.4–16.7)	2.97 (1.2–14.6)	0.005**
SUV_{max}-LN/LiBG	1.84 (0.81–9.83)	3.59 (1.39–9.83)	1.80 (0.81–9.30)	0.055
MTV-LN (mL)	12.16 (2.69–151.3)	28.71 (3.83–57.62)	9.325 (2.69–151.3)	0.018*
TLG-LN (mL)	16.37 (2.02–777.62)	83.31 (6.83–213.30)	12.72 (2.02–777.62)	0.015*
SUV_{max}-Li	2.05 (1.29–12.46)	2.34 (1.73–12.46)	1.775 (1.29–6.15)	0.069
SUV_{max}-Li/M	2.32 (0.93–16.31)	2.44 (1.76–16.31)	2.165 (0.93–4.52)	0.317
MTVc-Li (mL)	942.10 (568.42–1590.43)	1113.97 (686.68–1590.43)	932.385 (568.42–1482.97)	0.274
TLGc-Li (mL)	1268.14 (648.65–4947.97)	1711.83 (987.11–4947.97)	1201.855 (648.65–2224.83)	0.069
SUV_{max}-Sp	2.21 (1.27–8.02)	3.27 (1.50–8.02)	2.155 (1.27–4.55)	0.234
SUV_{max}-Sp/M	2.32 (0.91–13.59)	3.41 (1.29–13.59)	2.17 (0.91–4.1)	0.234
SUV_{max}-Sp/ LiBG	1.43 (0.81–3.19)	1.60 (0.81–3.19)	1.415 (1.00–2.45)	0.729

(Continued)

TABLE 1 | Continued

Parameters	Total ($N = 29$)	M-HLH ($N = 9$)	NM-HLH ($N = 20$)	*P*-value
MTVc-Sp (mL)	407.9 (144.35–1392.31)	659.29 (351.51–1392.31)	354.295 (144.35–1534.1)	0.011*
TLGc-Sp (mL)	661.44 (188.63–3614.05)	1307.57 (394.32–3614.05)	529.99 (188.63–2784.64)	0.011*
SUV_{max}-BM	3.39 (1.78–9.02)	3.60 (2.03–9.02)	3.22 (1.78–8.53)	0.167
SUV_{max}-BM/M	3.86 (1.28–15.28)	3.89 (1.86–15.28)	3.82 (1.28–6.27)	0.694
SUVmax-BM/LiBG	2.05 (1.10–4.25)	1.80 (1.10–4.04)	2.06 (1.31–4.25)	0.444

*HLH, hemophagocytic lymphohistiocytosis; EBV, Epstein-Barr virus; M-HLH, EBV-induced malignancy-associated HLH; NM-HLH, EBV-induced non-malignancy-associated HLH; EBV-HLH, HLH driven by pure EBV infection; CAEBV, chronic active EBV infection; LPD, lymphoproliferative disorders; HL, Hodgkin's Lymphoma; NHL, non-Hodgkin's lymphoma; ANC, absolute neutrophil count; Hb, hemoglobin; PLT, platelet; TG, triglyceride; sCD25, soluble CD25; NK, natural killer; IFN-γ, interferon-γ; TNF-α, tumor necrosis factor-α, IL: interleukin; ALT, alanine transaminase; AST, aspartate aminotransferase; LDH, lactate dehydrogenase; ESR, Erythrocyte Sedimentation Rate; CRP, C-reactive protein; Li, liver; Sp, spleen; BM, bone marrow; LN, lymph nodes; LiBG, liver background; M, mediastinum; SUV_{max}, maximum standard uptake value; MTV, metabolic tumor volume; TLG, total lesion glycolysis; c, corrected. *P < 0.05, **P < 0.01.*

were calculated to determine the optimal cut-off value. In univariate analysis of OS, the Kaplan-Meier method and log-rank test were used. The Cox proportional hazards model was used for the multivariate analysis of OS. In univariate analysis, $P < 0.02$ was considered statistically significant, and $P < 0.05$ was considered statistically significant in other condition. $^{\#}P < 0.02$, $^{*}P < 0.05$, $^{**}P < 0.01$.

RESULTS

Patients' Characteristics

A total of 29 children aged 1–16 years (median age, 7 years, male: female = 1:1.1) were enrolled in this study. All children were diagnosed by pathological examination. There were 20 cases in NM-HLH group (including nine cases of EBV-HLH and 11 cases of LPD grade 1–2) and nine cases in M-HLH group (including four cases of LPD grade 3 and 5 cases of lymphoma) (**Figure 1**). The general information and laboratory parameters are listed in **Table 1**.

Diagnostic Performance of ^{18}F-FDG PET/CT for Detecting M-HLH

In qualitative and visual analysis, almost all M-HLH children had lymphoma-like presentation in ^{18}F-FDG PET/CT, including multiple enlarged lymph nodes with obviously increased FDG uptake, local mass of fused lymph nodes, and/or extronodal lesions, etc. (**Figure 2**). The presence of extranodal hypermetabolic lesions is helpful for differentiating M-HLH from NM-HLH ($P = 0.074$), and the involvement of multiple organs had better diagnostic performance ($P = 0.022$) (**Table 1**). The affected organs included spleen, liver, bone marrow, brain, lung, intestine, kidney, adrenal gland, skin, nasal mucosa, muscle, etc. Five of the six patients of NM-HLH with extranodal lesions had only single organ involvement, including bone marrow involvement in one patient with EBV-HLH, spleen, bone marrow, adrenal gland, or muscles involvement in four patients with LPD grade 1–2 (**Figure 3**).

The lymph nodes and lesions of M-HLH had higher FDG uptake than NM-HLH based on visual analysis (**Figures 2**, **3**). For example, two patients diagnosed as NHL, LPD grade 3, presented as multiple normal-size lymph nodes with obviously increased

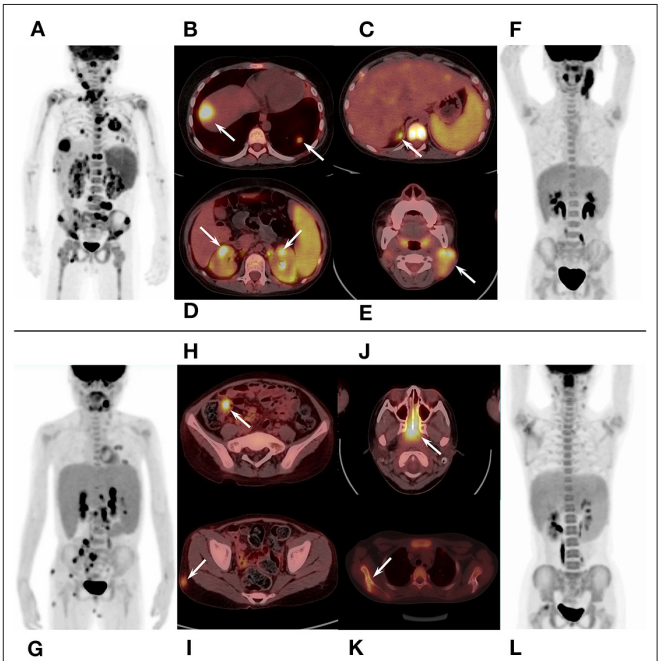

FIGURE 2 | ^{18}F-FDG PET/CT findings of M-HLH. **(A–D)** A 6-year-old boy with HL, had multiple enlarged hypermetabolic lymph nodes and extronodal hypermetabolic lesions in multiple organs (nasal mucosa, liver, lung, adrenal gland, kidney, and bone marrow). **(E,F)** A 6-year-old boy with LPD grade 3, had local mass of fused lymph nodes in the neck; **(G–I)**, a 10-year-old girl with NHL, had multiple enlarged hypermetabolic lymph nodes and extronodal hypermetabolic lesions in terminal ileum and skin. **(J–L)** A 10-year-old girl with NHL, had hypermetabolic lesions in nasopharynx and multiple lesions in scapula and femur. HLH, hemophagocytic lymphohistiocytosis; M-HLH, EBV-induced malignancy-associated HLH; LPD, lymphoproliferative disorders; HL, Hodgkin's Lymphoma; NHL, non-Hodgkin's lymphoma.

FDG uptake. And almost all the NM-HLH patients with enlarged lymph nodes (8/9), mostly LPD grade 1–2, had lower FDG uptake than M-HLH.

Then the quantitative and semi-quantitative analysis were inducted, and the level of age, SUV_{max}-lesions, SUV_{max}-LN, SUV_{max}-LN/M, MTV-LN, TLG-LN, MTVc-Sp and TLGc-Sp were significantly higher in M-HLH than in NM-HLH ($P =$ 0.004, 0.005, 0.004, 0.005, 0.018, 0.015, 0.011, 0.011, respectively,

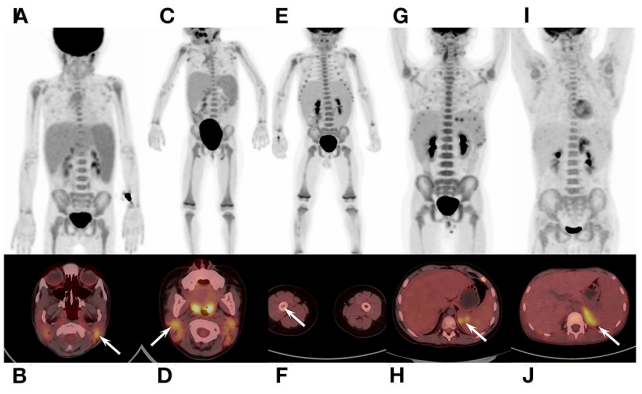

FIGURE 3 | ^{18}F-FDG PET/CT findings of NM-HLH. **(A,B)** A 5-year-old girl with EBV-HLH. **(C,D)** A 3-year-old girl with LPD grade 2. **(E,F)** a 2-year-old boy with LPD grade 1. **(G,H)** A 12-year-old boy with LPD grade 2. **(I,J)** A 11-year-old boy with LPD grade 2. NM-HLH patients usually show multiple lymph nodes with slightly or moderate increased FDG uptake, in bilateral cervical, mediastinal, axillary, retroperitoneal, pelvic and/or inguinal regions **(A–D,E,G,J)**, without extranodal organ involvement **(A,C)**. Sometimes, however, NM-HLH could show extranodal lesions in single organ, such as bone marrow **(F)**, spleen **(H)**, adrenal gland **(J)**, or muscles. HLH, hemophagocytic lymphohistiocytosis; EBV, Epstein-Barr virus; NM-HLH, EBV-induced non-malignancy-associated HLH; EBV-HLH, HLH driven by pure EBV infection; LPD, lymphoproliferative disorders.

Table 1; **Figures 4A–H**). However, there were no significant difference of the laboratory parameters and the other PET/CT findings between the two groups (**Table 1**).

The ROC curve analysis showed that the age, SUV_{max}-lesions, SUV_{max}-LN, SUV_{max}-LN/M, MTV-LN, TLG-LN, MTVc-Sp and TLGc-Sp were all able to differentiate M-HLH from NM-HLH with AUC of 0.833, 0.822, 0.828, 0.819, 0.778, 0.783, 0.794, 0.794, respectively (**Table 2**). SUV_{max}-LN/M (cut-off = 5.74) showed better performance than other parameters of lymph nodes and spleen, with high specificity (90%), low sensitivity (66.7%), and median accuracy (79.3%). Comparing to SUV_{max}-LN/M, SUV_{max}-lesions had higher sensitivity and accuracy, with the involving of the metabolic parameters of extranodal lesions (cut-off = 6.04, specificity = 90%, sensitivity = 77.8%, accuracy = 86.2%). The addition of combining variables might improve the diagnostic performance, with logistic regression method. Due to the linear correlation among the above PET parameters (variance inflation factor > 5), the age was combined with each PET parameter. Finally, combining the age with SUV_{max}-LN/M showed the best diagnostic efficiency, with increased specificity of 85% and sensitivity of 100% (AUC = 0.933) (**Table 2**; **Figure 4I**).

Correlation Analysis Between ^{18}F-FDG PET/CT Parameters and HLH Related Laboratory Parameters

In this study, the metabolic parameters of spleen and bone marrow correlated with the laboratory parameters related to HLH (**Table 3**, other parameters were not listed). SUV_{max}-SP showed a low positive correlation with serum ferritin, TG, IFN-γ, IL-6 ($r = 0.432$, $P = 0.019$; $r = 0.374$, $P = 0.046$; $r = 0.492$, $P = 0.007$; $r = 0.452$, $P = 0.014$). SUV_{max}-SP/M had a low to moderate positive correlation with TG, sCD25 and IL-6 ($r = 0.370$, $P = 0.048$; $r = 0.374$, $P = 0.046$; $r = 0.514$, $P = 0.004$). SUV_{max}-BM had a moderate positive correlation with IFN-γ ($r = 0.515$, $P = 0.004$). SUV_{max}-BM/M had a low negative correlation with Hb ($r = -0.412$, $P = 0.026$).

Prognostic Analysis

After a median follow-up of 88 weeks (range 3–156 weeks), 4 (13.8%) patients died, including two died of severe infection and multiple organs failure, one died of liver failure and disseminated intravascular coagulation before transplantation, and one died of severe infection after transplantation.

The treatment response of patients was evaluated at the 2nd, 4th, 6th, and 8th week (25, 24, 23 and 22 patients, respectively). The study found that the older age, increased TLGc-Sp, SUV_{max}-BM, SUV_{max}-LN, SUV_{max}-lesions, and the existence of serous effusion were related to the poorer treatment response at the 2nd week (not reaching partial remission) ($P = 0.03$, 0.048, 0.007, 0.031, 0.014, 0.036, respectively). Older age, increased SUV_{max}-LN, SUV_{max}-lesions, and the existence of serous effusion were related to the poorer treatment response at the 4th week ($P = 0.003$, 0.047, 0.001, 0.047, respectively). The treatment response of the 6th and 8th week were not analyzed as there were few patients reaching partial remission (three and four patients, respectively).

In the prediction of OS, the univariate analysis showed that the elevated metabolic parameters of the spleen, lymph nodes, and lesions, including SUV_{max}-lesions, SUV_{max}-LN, SUV_{max}-LN/LiBG, SUV_{max}-Sp, SUV_{max}-Sp/M, SUV_{max}-Sp/LiBG, and the level of IL-6, were prognostic factors ($P < 0.001$, $P = 0.011$, 0.019, 0.005, 0.016, 0.001, 0.018, respectively, **Table 4**). As the linear correlation among the metabolic parameters of the spleen or of the lymph nodes, only the parameters with the smallest P value were enrolled in multivariate analysis. Besides, the previous studies had reported that malignancy was a prognostic factor. Therefore, five parameters including malignancy, IL-6, SUV_{max}-lesions, SUV_{max}-Sp/LiBG, and SUV_{max}-LN were analyzed. Finally, the multivariate analysis showed that only SUV_{max}-lesions and SUV_{max}-Sp/LiBG were independent prognostic factors (cut-off = 7.66, $P = 0.025$; cut-off = 2.01, $P = 0.036$) (**Table 4**; **Figure 5**).

DISCUSSION

It is quite important to distinguish M-HLH from NM-HLH, and to find other prognostic factors for pediatric HLH with EBV infection. For children with M-HLH and poor prognosis, it's necessary to take more active and earlier treatments, such as chemotherapy and hematopoietic stem cell transplant, which might improve the prognosis (6, 20). The present study found that SUV_{max}-lesions, SUV_{max}-LN/M, and the union of age and SUV_{max}-LN/M had better diagnostic performance in differentiating M-HLH from NM-HLH. Besides, the presence of extranodal hypermetabolic lesions in multiple organs indicated the M-HLH. Moreover, ^{18}F-FDG PET/CT parameters of the spleen and bone marrow correlated with some parameters related to the activity of HLH. The multivariate analysis showed that

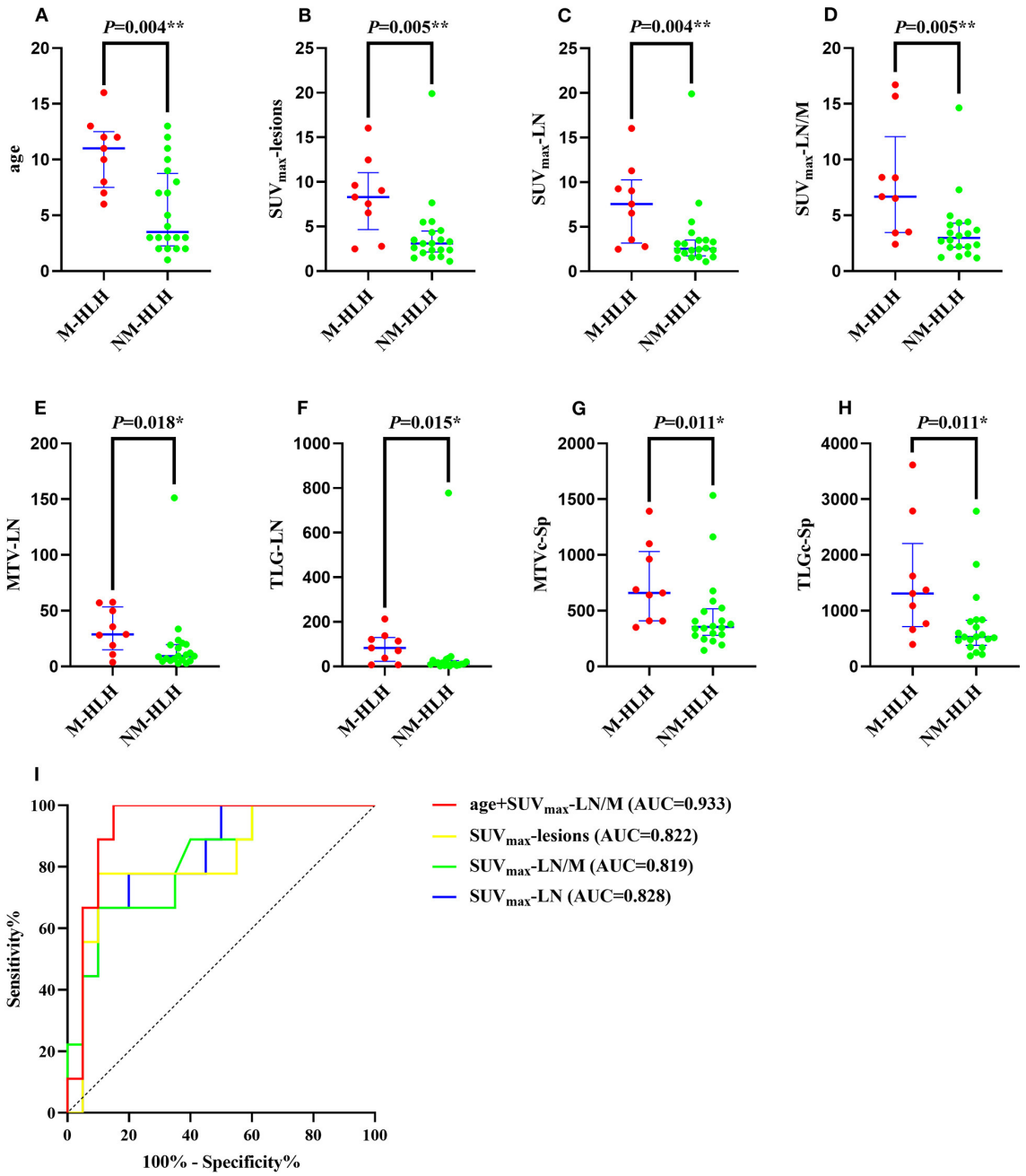

FIGURE 4 | Diagnostic ability of metabolic and volumetric parameters of ^{18}F-FDG PET/CT in differentiating M-HLH from NM-HLH. The age **(A)**, SUV_{max}-lesions **(B)**, SUV_{max}-LN **(C)**, SUV_{max}-LN/M **(D)**, MTV-LN **(E)**, TLG-LN **(F)**, MTVc-Sp **(G)**, TLGc-Sp **(H)** were significantly higher in M-HLH than NM-HLH ($P = 0.004$, 0.005, 0.004, 0.005, 0.018, 0.015, 0.011, 0.011, respectively). Receiver operating characteristic curve indicated that the combination of age and SUV_{max}-LN/M had the best diagnostic performance in differentiating M-HLH from NM-HLH (**I**, red line). Besides, SUV_{max}-lesions was better than SUV_{max}-LN and SUV_{max}-LN/M, with higher sensitivity and accuracy (**I**, yellow line). HLH, hemophagocytic lymphohistiocytosis; EBV, Epstein-Barr virus; M-HLH, EBV-induced malignancy-associated HLH; NM-HLH, EBV-induced non-malignancy-associated HLH; SUV_{max}, maximum standard uptake value; MTV, metabolic tumor volume; TLG, total lesion glycolysis; Sp, spleen; LN, lymph nodes; M, mediastinum; c, corrected; AUC, area under the curve. $^*P < 0.05$, $^{**}P < 0.01$.

the SUV_{max}-lesions > 7.66 and SUV_{max}-Sp/LiBG > 2.01 were independent prognostic factors for OS.

There are no characteristic findings on ^{18}F-FDG PET/CT in pediatric HLH with EBV infection. And the main purpose of using ^{18}F-FDG PET/CT is to find neoplastic lesions in lymph nodes or extranodal organs and to guide biopsies (6). The general findings usually indicate high inflammatory status, including hepatomegaly and splenomegaly with elevated FDG

TABLE 2 | Diagnostic ability of metabolic and volumetric parameters of ^{18}F-FDG PET/CT in differentiating M-HLH from NM-HLH.

Parameters	Cut-off values	Sensitivity (%)	Specificity (%)	Accuracy (%)	AUC (95%CI)
age	5.5	100.0	60.0	100.0	0.833 (0.688–0.979)
SUV_{max}-lesions	6.04	77.8	90.0	86.2	0.822 (0.648–0.996)
SUV_{max}-LN	6.04	66.7	90.0	58.6	0.828 (0.670–0.985)
SUV_{max}-LN/M	5.74	66.7	90.0	79.3	0.819 (0.656–0.983)
MTV- LN	25.82	66.7	90.0	79.3	0.778 (0.575–0.981)
TLG-LN	37.33	77.8	90.0	86.2	0.783 (0.567–1.000)
MTVc-Sp	407.15	88.9	65.0	93.1	0.794 (0.630–0.959)
TLGc-Sp	630.01	88.9	65.0	93.1	0.794 (0.614–0.975)
Age + SUV_{max}-lesions	/	100.0	85.0	/	0.911 (0.802–1.000)
Age + SUV_{max}-LN	/	100.0	80.0	/	0.906 (0.796–1.000)
Age + SUV_{max}-LN/M	/	100.0	85.0	/	0.933 (0.838–1.000)
Age + TLG-LN	/	66.7	85.0	/	0.839 (0.693–0.985)
Age + TLGc-Sp	/	77.8	90.0	/	0.883 (0.760–1.000)

AUC, area under the curve; CI, confidence interval; HLH, hemophagocytic lymphohistiocytosis; EBV, Epstein-Barr virus; M-HLH, EBV-induced malignancy-associated HLH; NM-HLH, EBV-induced non-malignancy-associated HLH; Sp, spleen; LN, lymph nodes; M, mediastinum; SUV_{max}, maximum standard uptake value; MTV, metabolic tumor volume; TLG, total lesion glycolysis; c, corrected.

TABLE 3 | Correlation analysis between ^{18}F-FDG PET/CT parameters and HLH related laboratory parameters.

Laboratory parameters	SUV_{max}-SP	SUV_{max}-SP/M	SUV_{max}-BM	SUV_{max}-BM/M
Hb (g/L)	−0.141 (0.466)	−0.287 (0.131)	−0.300 (0.114)	−0.412 (0.026)*
Serum ferritin (ng/mL)	0.432 (0.019)*	0.342 (0.069)	0.235 (0.220)	0.118 (0.541)
TG (mmol/L)	0.374 (0.046)*	0.370 (0.048)*	−0.047 (0.810)	−0.087 (0.654)
sCD25 (pg/mL)	0.367 (0.050)	0.374 (0.046)*	0.199 (0.300)	0.126 (0.515)
IFN-γ (pg/mL)	0.492 (0.007)**	0.330 (0.080)	0.515 (0.004)**	0.340 (0.071)
IL-6 (pg/mL)	0.452 (0.014)*	0.514 (0.004)**	0.272 (0.154)	0.268 (0.160)

*HLH, hemophagocytic lymphohistiocytosis; Hb, hemoglobin; TG, triglyceride; sCD25, soluble CD25; IFN-γ, interferon-γ; IL: interleukin; SUV_{max}, maximum standard uptake value; Sp, spleen; BM, bone marrow; M, mediastinum. *P < 0.05, **P < 0.01.*

uptake, diffuse elevated FDG uptake in the bone marrow, and serous effusion (21). In our study, there were also multiple lymphadenomegaly and extranodal lesions with increased FDG uptake except for the above findings. The extranodal involved organs included spleen, liver, bone marrow, brain, lung, intestine, kidney, adrenal gland, skin, nasal mucosa, and muscle, etc.

TABLE 4 | Univariate and multivariate analysis for overall survival in pediatric HLH with EBV infection.

Variables	Univariate analysis		Multivariate analysis	
	X^2	*P*-value	HR (95%CI)	*P* -value
Malignancy (yes)	5.157	0.023	-	-
IL-6 (>26.5 pg/mL)	5.645	0.018#	-	-
SUV_{max}-lesions (>7.66)	12.950	<0.001**	20.336 (1.460–283.191)	0.025*
SUV_{max}-LN (>3.31)	6.440	0.011#	-	-
SUV_{max}-LN/LiBG (>2.62)	5.499	0.019#	/	/
SUV_{max}-Sp (>3.13)	7.733	0.005#	/	/
SUV_{max}-Sp/M (>2.96)	5.826	0.016#	-	-
SUV_{max}-Sp/LiBG (>2.01)	10.619	0.001**	15.136 (1.187–192.952)	0.036*

HLH, hemophagocytic lymphohistiocytosis; EBV, Epstein-Barr virus; IL: interleukin; Sp, spleen; LN, lymph nodes; LiBG, liver background; M, mediastinum; SUV_{max}, maximum standard uptake value.
*#P < 0.02, *P < 0.05, **P < 0.01.*

In the visual differential diagnosis in pediatric HLH with EBV infection, this study found that lymphoma-like presentation, including multiple enlarged lymph nodes with obviously increased FDG uptake, local mass of fused lymph nodes, and/or extronodal lesions especially in multiple organs, could indicate the M-HLH. However, enlarged lymph nodes are common in NM-HLH patients, such as infectious mononucleosis and LPD grade 1–2 (22, 23). Therefore, it is important to consider the size, metabolism, and anatomical changes of lymph nodes comprehensively. On the contrary, some kinds of lymphoma do not show enlarged lymph nodes, such as EBV associated extranodal NK/T cell lymphoma, mainly affecting extranodal tissue, which is common in Asia (24). A previous study reported that hypermetabolic lesions in extranodal organs, such as liver, spleen and bone marrow, often indicated the involvement of HL and invasive NHL (25). Hence, the presence of extranodal hypermetabolic lesions, especially in multiple extranodal organs, was of great significance in the diagnosis of M-HLH. And it was consistent with previous studies, which suggested single extranodal organ involvement sometimes indicated NM-HLH (23, 26–28).

The present study found that semi-quantitative measurement of metabolic parameters of lymph nodes and extranodal organs might be helpful in distinguishing M-HLH from NM-HLH. It's reported that the FDG uptake of lymph nodes is related with invasiveness of the disease (29). Okano et al. found that increased SUV_{max}-LN and SUV_{max}-lesions indicated the lymphoma-associated HLH with cut-off value of 3.3, 5.5, respectively (21).

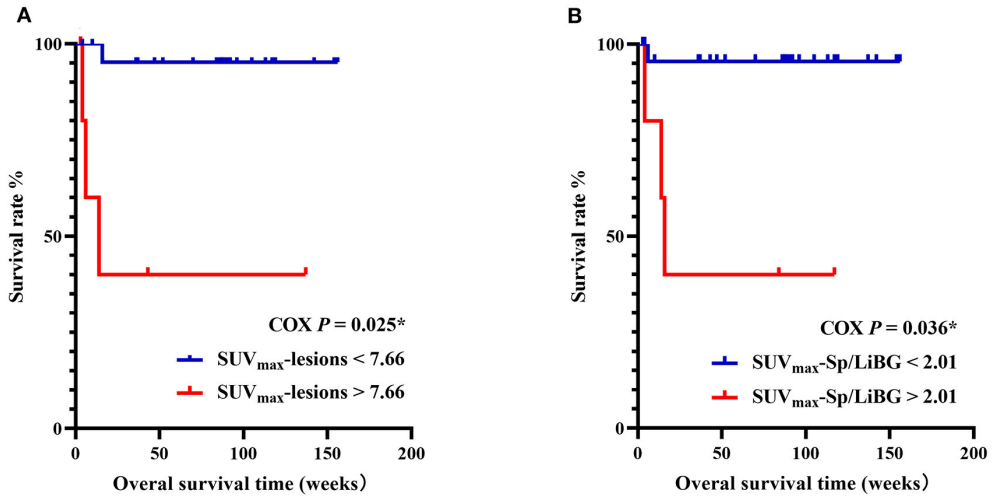

FIGURE 5 | Kaplan–Meier survival curves of pediatric HLH with EBV infection, with SUV_{max}-lesions **(A)**, SUV_{max}-Sp/LiBG **(B)**. In multivariate analysis, SUV_{max}-lesions > 7.66 and SUV_{max}-Sp/LiBG > 2.01 were independent prognostic factors for overall survival ($P = 0.025$, $P = 0.036$, respectively). HLH, hemophagocytic lymphohistiocytosis; EBV, Epstein-Barr virus; SUV_{max}, maximum standard uptake value; Sp, spleen; LiBG, liver background. * $P < 0.05$.

In the study, the level of FDG uptake of the lymph nodes and extranodal lesions, including SUV_{max}-LN, SUV_{max}-LN/M, MTV-LN, TLG-LN, and SUVmax-lesions, could help determine M-HLH. The best cut-off value of SUV_{max}-LN and SUV_{max}-lesions were both 6.04, which were higher than in adults, and it might be resulted from the physiological increased uptake of cervical lymph nodes in children (30). Comparing to SUV_{max}-LN and SUV_{max}-LN/M, the study showed that SUV_{max}-lesions had similar AUC and higher sensitivity and accuracy in detecting M-HLH, which indicated that the addition of the metabolic information of extranodal lesions could help finding the M-HLH better. In addition, it's reported that elder children are more likely to develop M-HLH with EBV infection (28). So age was combined with the above metabolic parameters separately in the differentiation analysis in our study. And we found that the combination of age and SUV_{max}-LN/M performed best. A study reported that some laboratory parameters, such as fibrinogen < 1.5g/L, PLT < 40g/L and LDH > 100U/L, were helpful in finding M-HLH (31). In our study, however, there was no significant difference in laboratory results between M-HLH and NM-HLH.

Due to the diversity and heterogeneity of pathology in EBV-associated disease, varying from LPD grade 1–3 to lymphoma, ^{18}F-FDG PET/CT is recommend to find the possible neoplastic lesions and to determine the most appropriate biopsy site according to the metabolic and anatomic information (6). However, it's important for physicians to note the following tips in using PET/CT scans. Firstly, physicians should adequately consider the radiation dose for children, identify those who really need the scan by preliminary screening examination, such as ultrasound. Moreover, physicians should be aware of the limitations of ^{18}F-FDG PET/CT, for example, false positive conditions in the Waldeyer's ring and gastrointestinal tract, and false negative conditions in mantle cell lymphoma and peripheral T-cell lymphoma (32). Furthermore, it's important to know that pathological biopsy is still the gold standard in differential diagnosis. In the study, one patient with T-cell NHL demonstrated as non-malignancy disease on PET/CT, only showing slightly increased FDG uptake in bone marrow. Besides, one NM-HLH patient mimicked the lymphoma on PET/CT, with multiple enlarged and hypermetabolic lymph nodes, and extranodal lesions in multiple organs (liver, bone marrow and lungs), which finally proved to be LPD grade 2.

The present study indicated that FDG uptake of the spleen and bone marrow might correlate with the inflammation of the body and the activity of HLH (33). Some laboratory parameters, including serum ferritin, TG, sCD25, IFN-γ, IL-6, IL-10 and TNF-α, could reflect the level of "inflammatory storm, which lead to the "sepsis-like symptoms" and organs injuries in HLH (34–36). It's reported that IFN-γ plays an essential role in the procedure, promoting the activation of mononuclear macrophages and resulting in hemophagocytosis (13). Yang et al. found that IL-6 seemed to play a similar but weaker role in causing organ damage than IFN-γ (34). In this study, the level of FDG uptake of the spleen positively correlated with IFN-γ and IL-6, which was consistent with previous studies. Besides, the metabolism of the bone marrow could reflect the hematopoiesis in it, because of its negative correlation with hemoglobin.

^{18}F-FDG PET/CT parameters could predict the treatment response and OS in pediatric HLH with EBV infection, which were rarely studied in the previous studies. The present study showed that older age, higher SUV_{max}-LN, and SUV_{max}-lesions indicated worse therapeutic effect at early treatment evaluation at the 2nd and 4th week, for they were related to M-HLH. And the higher FDG uptake of the spleen and bone marrow might indicated worse therapeutic effect at the 2nd week, for they were related to higher inflammatory status.

Our study found that SUV_{max}-Sp/LiBG and SUV_{max}-lesions were independent prognostic factors in HLH with EBV infection children. The cut-off value of SUV_{max}-Sp/LiBG (2.01) was higher than Kim's study in adult (1.19) (37). Kim et al. also suggested

that elevated SUV_{max}-BM, SUV_{max}-Sp, SUV_{max}-BM/LiBG were related to poorer prognosis (37). Besides, Zheng et al. reported that treatment strategy, serum fibrinogen and SUV_{max}-Sp/M were independent prognostic factors (14). The elevated FDG uptake of spleen is reported to be resulted from the activation of T cells and macrophages stimulated by IFN-γ (38). In other disease, Xia et al. retrospectively analyzed 141 patients with extranodal NK/T lymphoma and found that SUVmax-lesions ≥ 9.65 was associated with poor prognosis (39).

In the study, the univariate analysis also showed that the metabolic parameters of lymph nodes and IL-6 were related to OS. The baseline SUV_{max}, TLG and MTV of lymph nodes were related to OS in lymphoma, including HL, diffuse Large B-cell lymphoma, follicular lymphoma, peripheral T lymphocyte lymphoma, extranodal NK/T lymphoma, etc. (11, 40). Besides, elevated IL-6 indicates strong "inflammatory storm," suggesting the internal environment disturbance and a high mortality rate. Lu et al. found that IL-6 ≥ 18.59 pg/mL was one of the independent prognostic factors in 155 adults with HLH (41). Chen et al. found that IL-6 and IL-10 were prognostic factors in children with CAEBV (9). In the study, we did not find the relationship between volumetric parameters of lymph nodes and prognosis, which might because of the small sample size.

There were some limitations in this retrospective study. Firstly, due to the insufficient sample size, there were no verification group. Secondly, despite using pathology as a standard reference, differentiation between different pathologic types remains challenging. In the future, studies with large sample size in multicenter are needed to evaluate the value of ^{18}F-FDG PET/CT in pediatric HLH with EBV infection.

CONCLUSION

In conclusion, the study finds that ^{18}F-FDG PET/CT plays a certain role in pediatric HLH with EBV infection. M-HLH should be considered when SUV_{max}-lesions > 6.04, SUV_{max}-LN/M > 5.74 and the presence of extranodal hypermetabolic lesions in multiple organs. The FDG uptake of the spleen and bone marrow correlates with the activity of HLH. SUV_{max}-lesions > 7.66 and SUV_{max}-Sp/LiBG > 2.01 are independent prognostic factors for OS in pediatric HLH with EBV infection.

DATA AVAILABILITY STATEMENT

The original contributions presented in the study are included in the article, further inquiries can be directed to the corresponding authors.

AUTHOR CONTRIBUTIONS

XL and AW: conception and design of the study, protocol development, analysis, interpretation of data, and drafting the article. XY and JL: analysis and interpretation of data and revision of the article. SL: data collection. YK and WW: formal analysis. JY and RZ: project administration. All authors contributed to the article and approved the submitted version.

FUNDING

This work was supported by the National Natural Science Foundation of China (Nos. 81771860 and 81971642), Beijing Natural Science Foundation (No. 7192041), National Key Research and Development Plan (No: 2020YFC0122000), National Science and Technology Key Projects (No. 2017ZX09304029001) and the Pediatric Medical Coordinated Development Centre of Beijing Municipal Administration of Hospitals (No. XTZD20180202).

ACKNOWLEDGMENTS

We thank Yuxin Zhao, Beijing Friendship Hospital Affiliated to Capital Medical University, for the valuable discussions on statistical analyses.

REFERENCES

1. Al-Samkari H, Berliner N. Hemophagocytic lymphohistiocytosis. *Annu Rev Pathol.* (2018) 13:27–49. doi: 10.1146/annurev-pathol-020117-043625
2. Ramos-Casals M, Brito-Zerón P, López-Guillermo A, Khamashta MA, Bosch X. Adult haemophagocytic syndrome. *Lancet.* (2014) 383:1503–16. doi: 10.1016/S0140-6736(13)61048-X
3. Okano M, Gross TG. Acute or chronic life-threatening diseases associated with Epstein-Barr virus infection. *Am J Med Sci.* (2012) 343:483–89. doi: 10.1097/MAJ.0b013e318236e02d
4. Ishii E. Hemophagocytic lymphohistiocytosis in children: pathogenesis and treatment. *Front Pediatr.* (2016) 4:47. doi: 10.3389/fped.2016.00047
5. Xu X-J, Wang H-S, Ju X-L, Xiao P-F, Xiao Y, Xue H-M, et al. Clinical presentation and outcome of pediatric patients with hemophagocytic lymphohistiocytosis in China: a retrospective multicenter study. *Pediatr Blood Cancer.* (2017) 64:1–6. doi: 10.1002/pbc.26264
6. El-Mallawany NK, Curry CV, Allen CE. Haemophagocytic lymphohistiocytosis and Epstein-Barr virus: a complex relationship with diverse origins, expression and outcomes. *Br J Haematol.* (2022) 196:31—44. doi: 10.1111/bjh.17638
7. Ohshima K, Kimura H, Yoshino T, Kim CW, Ko YH, Lee S-S, et al. Proposed categorization of pathological states of EBV-associated T/natural killer-cell lymphoproliferative disorder (LPD) in children and young adults: overlap with chronic active EBV infection and infantile fulminant EBV T-LPD. *Pathol Int.* (2008) 58:209–17. doi: 10.1111/j.1440-1827.2008.02213.x
8. Kim WY, Montes-Mojarro IA, Fend F, Quintanilla-Martinez L. Epstein-Barr virus-associated T and NK-cell lymphoproliferative diseases. *Front Pediatr.* (2019) 7:71. doi: 10.3389/fped.2019.00071
9. Chen S, Wei A, Ma H, Zhang L, Lian H, Zhao Y, et al. Clinical features and prognostic factors of children with chronic active epstein-barr virus infection: a retrospective analysis of a single center. *J Pediatr.* (2021) 238:268–74.e2. doi: 10.1016/j.jpeds.2021.07.009
10. El-Galaly TC, Villa D, Gormsen LC, Baech J, Lo A, Cheah CY. FDG-PET/CT in the management of lymphomas: current status and future directions. *J Intern Med.* (2018) 284:358–76. doi: 10.1111/joim.12813

11. Feng X, Wen X, Li L, Sun Z, Li X, Zhang L, et al. Baseline total metabolic tumor volume and total lesion glycolysis measured on 18F-FDG PET-CT predict outcomes in T-cell lymphoblastic lymphoma. *Cancer Res Treat.* (2021) 53:837–46. doi: 10.4143/crt.2020.123
12. Sin KM, Ho SKD, Wong BYK, Gill H, Khong P-L, Lee EYP. Beyond the lymph nodes: FDG-PET/CT in primary extranodal lymphoma. *Clin Imaging.* (2017) 42:25–33. doi: 10.1016/j.clinimag.2016.11.006
13. Canna SW, Marsh RA. Pediatric hemophagocytic lymphohistiocytosis. *Blood.* (2020) 135:1332–43. doi: 10.1182/blood.2019000936
14. Zheng Y, Hu G, Liu Y, Ma Y, Dang Y, Li F, et al. The role of F-FDG PET/CT in the management of patients with secondary haemophagocytic lymphohistiocytosis. *Clin Radiol.* (2016) 71:1248–54. doi: 10.1016/j.crad.2016.05.011
15. Lai W, Wang Y, Wang J, Wu L, Jin Z, Wang Z. Epstein-Barr virus-associated hemophagocytic lymphohistiocytosis in adults and adolescents-a life-threatening disease: analysis of 133 cases from a single center. *Hematology.* (2018) 23:810–16. doi: 10.1080/10245332.2018.1491093
16. Henter J-I, Horne A, Aricó M, Egeler RM, Filipovich AH, Imashuku S, et al. HLH-2004: Diagnostic and therapeutic guidelines for hemophagocytic lymphohistiocytosis. *Pediatr Blood Cancer.* (2007) 48: 124–31. doi: 10.1002/pbc.21039
17. Nafiu OO, Owusu-Bediako K, Chiravuri SD. Effect of body mass index category on body surface area calculation in children undergoing cardiac procedures. *Anesth Analg.* (2020) 130:452–61. doi: 10.1213/ANE.0000000000004016
18. Spijkers S, Littooij AS, Nievelstein RAJ. Measurements of cervical lymph nodes in children on computed tomography. *Pediatr Radiol.* (2020) 50:534–42. doi: 10.1007/s00247-019-04595-y
19. Marsh RA, Allen CE, McClain KL, Weinstein JL, Kanter J, Skiles J, et al. Salvage therapy of refractory hemophagocytic lymphohistiocytosis with alemtuzumab. *Pediatr Blood Cancer.* (2013) 60:101–09. doi: 10.1002/pbc.24188
20. Okano M, Kawa K, Kimura H, Yachie A, Wakiguchi H, Maeda A, et al. Proposed guidelines for diagnosing chronic active Epstein-Barr virus infection. *Am J Hematol.* (2005) 80:64–9. doi: 10.1002/ajh.20398
21. Zhang LJ, Xu J, Liu P, Ding CY Li JY, Qiu HX, et al. The significance of 18F-FDG PET/CT in secondary hemophagocytic lymphohistiocytosis. *J Hematol Oncol.* (2012) 5:40. doi: 10.1186/1756-8722-5-40
22. Dunmire SK, Verghese PS, Balfour HH. Primary Epstein-Barr virus infection. *J Clin Virol.* (2018) 102:84–92. doi: 10.1016/j.jcv.2018.03.001
23. Ørbæk M, Graff J, Markova E, Kronborg G, Lebech A-M. (18)F-FDG PET/CT Findings in acute Epstein-Barr virus infection mimicking malignant lymphoma. *Diagnostics (Basel).* (2016) 6:18. doi: 10.3390/diagnostics6020018
24. Tse E, Kwong Y-L. NK/T-cell lymphomas. *Best Pract Res Clin Haematol.* (2019) 32:253–61. doi: 10.1016/j.beha.2019.06.005
25. Barrington SF, Mikhaeel NG, Kostakoglu L, Meignan M, Hutchings M, Müeller SP, et al. Role of imaging in the staging and response assessment of lymphoma: consensus of the International Conference on Malignant Lymphomas Imaging Working Group. *J Clin Oncol.* (2014) 32: 3048-58. d doi: 10.1200/JCO.2013.53.5229
26. Pan Q, Luo Y, Wu H, Ma Y, Li F. Epstein-Barr virus-associated hemophagocytic lymphohistiocytosis mimicking lymphoma on FDG PET/CT. *Clin Nucl Med.* (2018) 43:125–27. doi: 10.1097/RLU.0000000000001923
27. Thomas DL, Syrbu S, Graham MM. Epstein-Barr virus mimicking lymphoma on FDG-PET/CT. *Clin Nucl Med.* (2009) 34:891–93. doi: 10.1097/RLU.0b013e3181bed135
28. Toriihara A, Nakajima R, Arai A, Nakadate M, Abe K, Kubota K, et al. Pathogenesis and FDG-PET/CT findings of Epstein-Barr virus-related lymphoid neoplasms. *Ann Nucl Med.* (2017) 31:425–36. doi: 10.1007/s12149-017-1180-5
29. Montes de Jesus F, Vergote V, Noordzij W, Dierickx D, Dierckx RAJO, Diepstra A, et al. Semi-quantitative characterization of post-transplant lymphoproliferative disorder morphological subtypes with [18F]FDG PET/CT. *J Clin Med.* (2021) 10:361. doi: 10.3390/jcm10020361
30. Vali R, Bakkari A, Marie E, Kousha M, Charron M, Shammas A, et al. uptake in cervical lymph nodes in children without head and neck cancer. *Pediatr Radiol.* (2017) 47:860–67. doi: 10.1007/s00247-017-3835-8
31. Li F, Li P, Zhang R, Yang G, Ji D, Huang X, et al. Identification of clinical features of Lymphoma-Associated Hemophagocytic Syndrome (LAHS): an analysis of 69 patients with hemophagocytic syndrome from a single-center in central region of China. *Med Oncol.* (2014) 31:902. doi: 10.1007/s12032-014-0902-y
32. Elstrom R, Guan L, Baker G, Nakhoda K, Vergilio JA, Zhuang H, et al. Utility of FDG-PET scanning in lymphoma by WHO classification. *Blood.* (2003) 101:3875–6. doi: 10.1182/blood-2002-09-2778
33. Yang YQ, Ding CY, Xu J, Fan L, Wang L, Tian T, et al. Exploring the role of bone marrow increased FDG uptake on PET/CT in patients with lymphoma-associated hemophagocytic lymphohistiocytosis: a reflection of bone marrow involvement or cytokine storm? *Leuk Lymphoma.* (2016) 57:291–98. doi: 10.3109/10428194.2015.1048442
34. Yang S-L, Xu X-J, Tang Y-M, Song H, Xu W-Q, Zhao F-Y, et al. Associations between inflammatory cytokines and organ damage in pediatric patients with hemophagocytic lymphohistiocytosis. *Cytokine.* (2016) 85:14–7. doi: 10.1016/j.cyto.2016.05.022
35. Kato J, Okamoto T, Motoyama H, Uchiyama R, Kirchhofer D, Van Rooijen N, et al. Interferon-gamma-mediated tissue factor expression contributes to T-cell-mediated hepatitis through induction of hypercoagulation in mice. *Hepatology.* (2013) 57:362–72. doi: 10.1002/hep.26027
36. Zoller EE, Lykens JE, Terrell CE, Aliberti J, Filipovich AH, Henson PM, et al. Hemophagocytosis causes a consumptive anemia of inflammation. *J Exp Med.* (2011) 208:1203–14. doi: 10.1084/jem.20102538
37. Kim J, Yoo SW, Kang SR, Bom HS, Song HC, Min JJ. Clinical implication of F-18 FDG PET/CT in patients with secondary hemophagocytic lymphohistiocytosis. *Ann Hematol.* (2014) 93:661–7. doi: 10.1007/s00277-013-1906-y
38. Takada H, Takahata Y, Nomura A, Ohga S, Mizuno Y, Hara T. Increased serum levels of interferon-gamma-inducible protein 10 and monokine induced by gamma interferon in patients with haemophagocytic lymphohistiocytosis. *Clin Exp Immunol.* (2003) 133:448–53. doi: 10.1046/j.1365-2249.2003.02237.x
39. Xia X, Wang Y, Yuan J, Sun W, Jiang J, Liu C, et al. Baseline SUVmax of 18F-FDG PET-CT indicates prognosis of extranodal natural killer/T-cell lymphoma. *Medicine.* (2020) 99:e22143. doi: 10.1097/MD.0000000000022143
40. Guo B, Tan X, Ke Q, Cen H. Prognostic value of baseline metabolic tumor volume and total lesion glycolysis in patients with lymphoma: a meta-analysis. *PLoS One.* (2019) 14:e0210224. doi: 10.1371/journal.pone.0210224
41. Lu M, Xie Y, Guan X, Wang M, Zhu L, Zhang S, et al. Clinical analysis and a novel risk predictive nomogram for 155 adult patients with hemophagocytic lymphohistiocytosis. *Ann Hematol.* (2021) 100:2181–93. doi: 10.1007/s00277-021-04551-7

Conflict of Interest: The authors declare that the research was conducted in the absence of any commercial or financial relationships that could be construed as a potential conflict of interest.

Publisher's Note: All claims expressed in this article are solely those of the authors and do not necessarily represent those of their affiliated organizations, or those of the publisher, the editors and the reviewers. Any product that may be evaluated in this article, or claim that may be made by its manufacturer, is not guaranteed or endorsed by the publisher.